Journal of
Materials Chemistry C

Accepted Manuscript

This article can be cited before page numbers have been issued, to do this please use: J. Ly, S. Lopez, J. B. Lin, J. Kim, H. Lee, E. K. Burnett, L. Zhang, A. Aspuru Guzik, K. N. Houk and A. Briseno, *J. Mater. Chem. C*, 2018, DOI: 10.1039/C7TC05775J.

ROYAL SOCIETY OF CHEMISTRY

rsc.li/materials-c

View Article Online
DOI: 10.1039/C7TC05775J

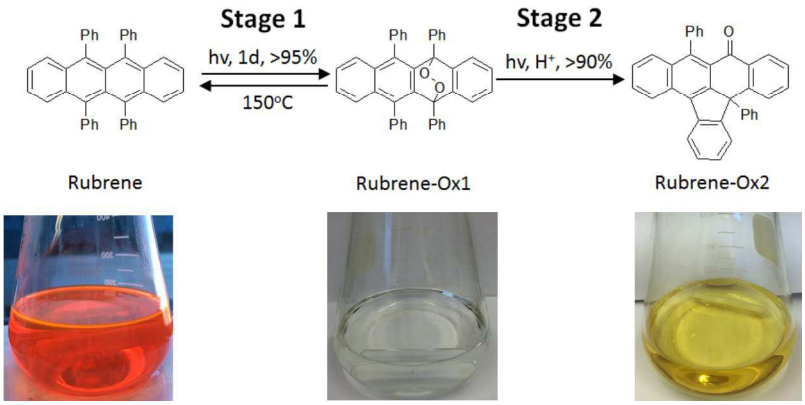

In the course of studying the formation and thermally activated cycloreversion of oxidized rubrene to pristine rubrene, we observed an irreversible, second stage oxidized product. Such impurities present in solution processed rubrene devices will detrimentally impact device performance and cannot be remediated through the application of heat to reform the parent acene. Devices from pure, thermally treated oxidized rubrene did in fact yield high carrier mobilities in both thin films and single crystal transistors. Understanding the formation of the irreversible adduct will help one design more chemically robust rubrene derivatives.

View Article Online
DOI: 10.1039/C7TC05775J

Journal Name

COMMUNICATION

Reversible and Irreversible Oxidation of Rubrene, and Implications for Device Stability

Received 00th January 20xx,
Accepted 00th January 20xx

DOI: 10.1039/x0xx00000x

www.rsc.org/

Jack T. Ly,[a] Steven A. Lopez,[b,c] Janice B. Lin,[b] JaeJoon Kim,[a] Hyunbuk Lee,[a] Edmund K. Burnett,[a] Lei Zhang,[*a,d] Alán Aspuru-Guzik,[c] K. N. Houk,[*b] and Alejandro L. Briseno[*a]

Dedicated to our esteemed friend and mentor, Fred Wudl

The rapid spontaneous photo-oxidation of rubrene to form endo-peroxide, rubrene-Ox1, was monitored via ^{1}H NMR and UV-Vis spectroscopy. The reaction is thermally reversible, which restores high mobility devices in both the crystalline thin film and single crystal. Prolonged stirring in chlorinated solvents yields a secondary, irreversible product, rubrene-Ox2, which has lost phenol, as confirmed by single crystal analysis. An acid-catalyzed rearrangement of the *endo*-peroxide to form rubrene-Ox2 was identified here with Density Functional Theory (DFT). Implications of the nature of these processes for the preparation of organic transistors are described.

Organic semiconductors (OSCs) have attracted interest in large-area devices due to their mechanical flexibility, solution processability, and performance that rivals that of amorphous silicon.[1–5] Although these materials appear as attractive candidates for next-generation semiconductor materials, their propensity to degrade under ambient conditions has hindered their commercial use. Even the benchmark organic semiconductor, rubrene, one of the best performing materials,[6–9] has been shown to readily oxidize in both solution and amorphous thin films.[10–16] The photo-oxidation of rubrene has been well documented,[16,17] involving the photosensitized formation of singlet oxygen and subsequent formation of the endo-peroxide Diels-Alder adduct.[18] In our efforts to monitor and clarify the photo-oxidation of rubrene[11,17,19,20] and its thermal cycloreversion,[21] we observed an irreversible second stage oxidation product, **rubrene-Ox2**. In addition, we describe an acid-catalyzed process that irreversibly destroys the active transport layer and leads to permanent degradation of device performance. Here, ^{1}H NMR and UV-Vis were utilized to monitor the thermal cycloreversion process of the oxidized species. The fidelity of this cycloreversion process to restore the intrinsic properties of rubrene was demonstrated via the fabrication of high mobility devices from previously oxidized rubrene. Prolonged photo-oxidation in $CHCl_3$ solution converts the endo-peroxide irreversibly to **rubrene-Ox2**. It should be noted that this secondary degradation product had been reported in 1955 [23] through an acid treatment of **rubrene-Ox1,** to form the same product we report here.[22–24] However, in that report, neither the mechanism of product formation nor the crystal structure were reported. Herein, we report the first crystal structure of **rubrene-Ox2,** and through quantum mechanical computations, propose an acid catalyzed *endo*-peroxide rearrangement mechanism for the generation of **rubrene-Ox2**.

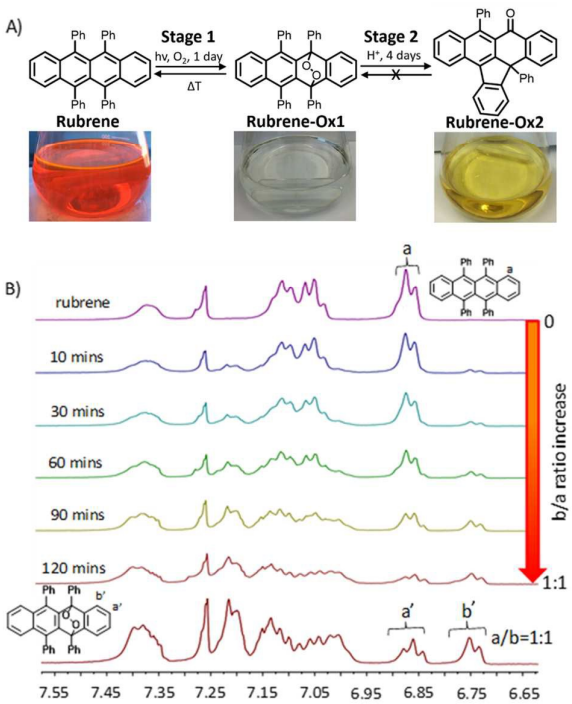

Figure 1. A) Molecular structure of rubrene, **rubrene-Ox1**, **rubrene-**

[a]*Department of Polymer Science and Engineering, University of Massachusetts Amherst, Amherst, Massachusetts 01003, USA. Email: abriseno@mail.pse.umass.edu*
[b]*Department of Chemistry and Biochemistry, University of California, Los Angeles, Los Angeles, California, 02138, USA. Email: houk@chem.ucla.edu*
[c]*Department of Chemistry and Chemical Biology, Harvard University, Cambridge, Massachusetts, 02138, USA.*
[d]*College of Energy, Beijing University of Chemical Technology, Beijing 100124, China. Email: zhl@mail.buct.edu.cn*

†Electronic Supplementary Information (ESI) available: Detailed synthetic procedures; UV-Vis of oxidation of rubrene and half-life calculations; ^{1}H NMR; CIF files of rubrene-Ox1 and rubrene-Ox2, and coordinates and energies for stationary points for rubrene-Ox1, strucutures 2-6, and rubrene-Ox2. DOI: 10.1039/x0xx00000x

View Article Online
DOI: 10.1039/C7TC05775J
COMMUNICATION Journal Na

Ox2. B) ^{1}H NMR oxidation process of rubrene and pure **rubrene-Ox1.**

Rubrene-Ox1 can be easily accessed in high yield (97%) by stirring a rubrene solution in chlorinated solvents under ambient laboratory conditions. All solution concentrations for this study were 2x10^{-5} M in chloroform. The formation of **rubrene-Ox1** was monitored using ^{1}H NMR (Figure 1) through the appearance of a new triplet and doublet peak at 6.86 and 6.75 ppm, respectively. After 120 minutes, full conversion to **rubrene-Ox1** was determined. The nmr spectrum matched that of separately purified **rubrene-Ox1**, shown in the bottom spectrum of Figure 1B. The characterization of rubrene-Ox1 is consistent with previously reported work.[25,26]

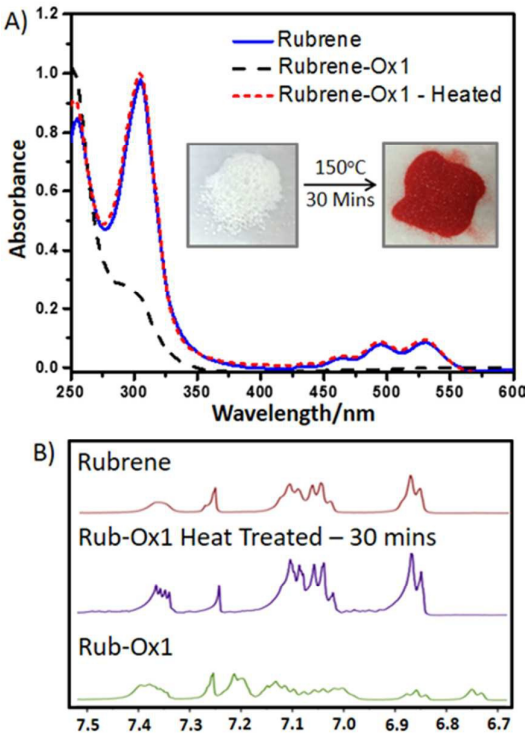

Figure 2. A) UV-Vis spectra of thin films of **rubrene-Ox1** heating at 150 °C for 30 mins (red), **rubrene-Ox1** (black), and rubrene (blue), and B) ^{1}H NMR spectra for pristine rubrene, heat treated **rubrene-Ox1**, and **rubrene-Ox1**.

The degradation profile of rubrene in solution was also investigated through UV-Vis absorption to complement ^{1}H NMR experiments. In solution and amorphous films, pristine rubrene has three signature absorption peaks at 529, 494, and 464 nm while **rubrene-Ox1** has no distinct peaks in the visible spectra range. UV-Vis measurements were carried out on both solution state and thin films of pristine rubrene and **rubrene-Ox1**. A rubrene half-life value of 26 minutes in solution was determined through the careful monitoring and depletion of the three distinct rubrene peaks under laboratory conditions (see Supporting Information). **Rubrene-Ox1** thin films were annealed to give cycloreversion to reform the parent rubrene. Upon heating the thin films of **rubrene-Ox1** at 150 °C, distinct absorption peaks of rubrene emerged within minutes. After 30 minutes of heating, the thin film spectrum of the thermally treated **rubrene-Ox1** sample matches that of pristine rubrene, displaying the efficiency of the thermolysis. Additionally, ^{1}H NMR spectra (Figure 2B) were collected for the thermolysis of **rubrene-Ox1** powder at the same temperature under a nitrogen atmosphere; cycloreversion approached full conversion in the first 10 minutes with the disappearance of the peroxide adduct peaks around 6.75 ppm. The bulk, white powder converted to a vibrant red color during this heating process.

The oxidation of rubrene can be monitored visually as the solution color changes from red to colorless. Stirring for four days results in a yellow solution, indicating that a subsequent reaction in chlorinated solvents occurred. A previous report observed similar results when treating a rubrene solution with CF_3COOH, yielding a yellow product, identified as indenonaphthacene.[27] That product, however, is a different structure from the compound observed here, and was not a product observed in our studies. The structure of the purified **rubrene-Ox2** was confirmed to be the structure shown via single crystal analysis and ^{1}H NMR (Figure 3). The crystal structure of **rubrene-Ox2** in Figure 3B shows that the molecular structure is related to indenonaphthacene with the exception of a ketone at the C-1 position in place of a phenyl substituent. This secondary rearrangement product also lost the elements of phenol. Prolonged photodegradation of rubrene was performed in a chloroform solution neutralized by Na_2CO_3. No observable yellow color was produced after 4 days; however, upon the addition of CH_3SO_3H, the solution immediately became yellow (see Supporting Information). The net loss of a phenol renders the process irreversible.

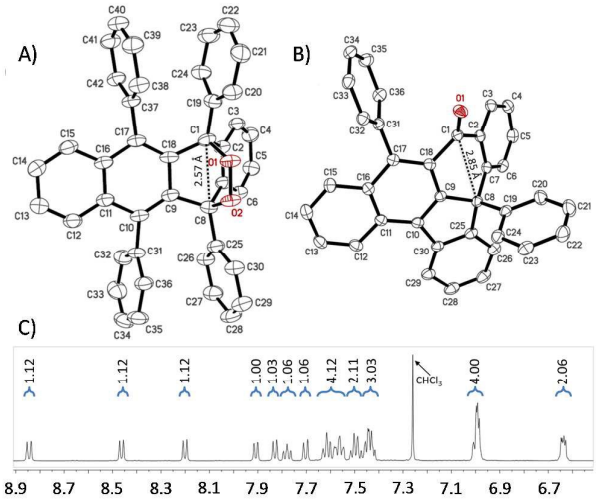

Figure 3. Crystal structures of, A) **rubrene-Ox1**, B) **rubrene-Ox2**, and C) ^{1}H NMR of **rubrene-Ox2**.

Figure 4 shows the proposed acid-catalyzed mechanism for rubrene *endo*-peroxide rearrangement to **rubrene-Ox2**. Chloroform is known to contain acidic impurities (HCl).[28] The proposed mechanism was evaluated using M06-2X/6-311+G(d,p)-IEFPCM^{CHCl3}//M06-2X/6-31G(d,p)-IEFPCM^{CHCl3} and B3LYP-D3BJ/6-IEFPCM^{CHCl3}calculations. Both methods predict the same mechanism, but the following discussion is based on the computed free energies relative to rubrene and $^3O_2$ using M06-2X/6-311+G(d,p)-IEFPCM^{CHCl3}//M06-2X/6-31G(d,p)-IEFPCM^{CHCl3}. The protonation of *endo*-peroxide **rubrene-Ox1** by model acid, H_3O^+, gives cation, **2.** The protonated *endo*-peroxide undergoes a ring opening to afford the stabilized carbocation **3**, which is 27.2 kcal mol^{-1} lower in energy than **2**. Attack of the cation at C-5 produces

View Article Online
DOI: 10.1039/C7TC05775J

Wheland intermediate **4**, which is higher in energy than **3** by 5.4 kcal mol^{-1}. Subsequent deprotonation of **4** by H_2O gives **5**, which rearranges via a [1,2]-Ph shift and dehydration to give **6**. Finally, **6** loses PhOH to afford the observed product, **rubrene-Ox2**.

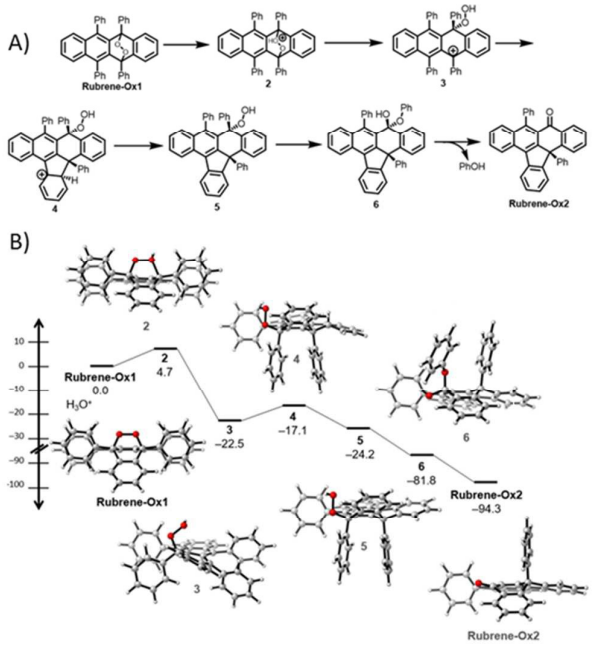

Figure 4. A) Proposed acid-catalyzed rearrangement mechanism. B) Computed free energies of the proposed mechanism of **rubrene-Ox1** rearrangement to **rubrene-Ox2** using M06-2X/6-311+G(d,p)-IEFPCM^{CHCl3}//M06-2X/6-31G(d,p)-IEFPCM^{CHCl3}.

Having established the structures of the rubrene oxidation products and the means and mechanisms of interconversions, we turned to exploration of device characteristics under different conditions. Although **rubrene-Ox2** is formed irreversibly, **rubrene-Ox1** could be a potential precursor to functional transistors. Known examples of acene precursors often employ light and or heat-sensitive sufinylacetamide and monoketone moieties to yield active semiconductors.[29–37] To evaluate the semiconductor properties of thermally recovered rubrene, we fabricated thin-films via spin casting from solution. Pristine rubrene and reduced rubrene from the *endo*-peroxide are annealed to form the orthorhombic crystals.[38] As shown in Figure 5a-c, pristine rubrene and reduced **rubrene-Ox1** show interfacing crystallites with different colors corresponding to the desired crystalline phase[39–42] while **rubrene-Ox1** instead exhibits an amorphous, featureless film. Transfer characteristics of each film are shown in Figure 5d. Pristine and reduced **rubrene-Ox1** showed hole mobility of 0.037 and 0.009 cm^2 V^{-1} s^{-1}, V_{th} of 16 and 13 V, and routine current on/off ratio of ~10^4 and ~10^3, respectively. While the mobilities are rather low, we produced the first example of additive-free solution-processed rubrene.[43,44] The lower mobility of reduced **rubrene-Ox1** may result from the presence of a **rubrene-Ox1** impurity post-thermolysis or structural disorder at the dielectric-semiconductor interface.

Finally, to demonstrate the reversibility of **rubrene-Ox1** oxidation, we carried out physical vapor transport experiments with bulk oxidized rubrene as the source material. This experiment was carried out at 300 °C in which two events occur: (1) the cycloreversion process, and (2) the sublimation of the reformed rubrene. It is interesting to note that the cycloreversion and sublimation occur in one step to produce large, ultrathin rubrene crystals with high purity. We fabricated single crystal transistors from these crystals and measured carrier mobilities approaching 1.5 cm^2 V^{-1} S^{-1}, with V_{th} of 3 V, and current on/off ratios of ~10^6. Figure 5E shows the transfer characteristics of the single crystal rubrene device. Output characteristics for the same device exhibits excellent current modulation when scanned from 0 to -40 V (see supporting information). These characteristics demonstrate that rubrene crystals grown from a **rubrene-Ox1** source can reproduce the fully conjugated form to yield high mobility transistors. This experiment clearly shows the reversibility of **rubrene-Ox1** to rubrene to form fully functional devices.

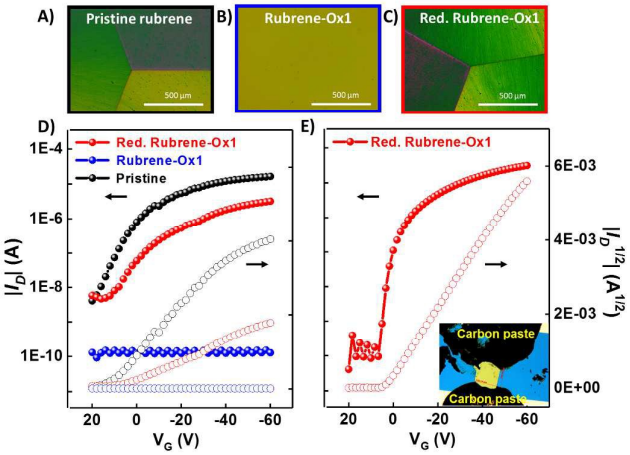

Figure 5. Polarized optical images of A) pristine rubrene, B) **rubrene-Ox1**, and C) reduced **rubrene-Ox1** crystalline thin films. Transfer characteristics of D) pristine rubrene, **rubrene-Ox1**, reduced **rubrene-Ox1** thin film transistors, and E) single crystal rubrene crystal transistor (grown from **rubrene-Ox1** source via PVT).

Conclusions

In the course of studying the formation and thermally activated cycloreversion of **rubrene-Ox1** to pristine rubrene, we observed an irreversible, second stage oxidized product - **rubrene-Ox2**. It was found that acid impurities in chlorinated solvents lead to a pyramidalized ketone derivative, which is inactive in organic transistors. Using DFT, we identify the lowest energy pathway to the acid catalyzed formation of this irreversible product. Such impurities present in solution processed rubrene devices will detrimentally impact device performance and cannot be remediated through the application of heat to reform the parent acene. Devices from pure, thermally treated **rubrene-Ox1** did in fact yield high carrier mobilities in both thin films and single crystal

DOI: 10.1039/C7TC05775J

transistors. Understanding the formation of the irreversible adduct will help us design more chemically robust rubrene derivatives.

ACKNOWLEDGMENT

J.L. and K.N.H. acknowledge funding from the National Science Foundation (DMR-1508627); L.Z. thanks the Office of Naval Research (N000147-14-1-0053) and Science Foundation of China (21672020). J.L and A.L.B acknowledge the National Science Foundation (DMR-1508627). S.A.L acknowledges the DOE EERE Postdoctoral fellowship for funding. A.A.-G. acknowledges the Department of Energy for support (DE-SC0015959). We thank Dr. Sean Parkin at the University of Kentucky for crystal structure analysis.

Notes and references

1 Y. Li, D. Ji, J. Liu, Y. Yao, X. Fu, W. Zhu, C. Xu, H. Dong, J. Li and W. Hu, Quick Fabrication of Large-area Organic Semiconductor Single Crystal Arrays with a Rapid Annealing Self-Solution-Shearing Method., *Sci. Rep.*, 2015, **5**, 13195.
2 A. L. Briseno, R. J. Tseng, M. M. Ling, E. H. L. Falcao, Y. Yang, F. Wudl and Z. Bao, High-performance organic single-crystal transistors on flexible substrates, *Adv. Mater.*, 2006, **18**, 2320–2324.
3 H. T. Yi, M. M. Payne, J. E. Anthony and V. Podzorov, Ultra-flexible solution-processed organic field-effect transistors, *Nat. Commun.*, 2012, **3**, 1259.
4 M. a. Reyes-Martinez, A. J. Crosby and A. L. Briseno, Rubrene crystal field-effect mobility modulation via conducting channel wrinkling, *Nat. Commun.*, 2015, **6**, 6948.
5 T. Sekitani, U. Zschieschang, H. Klauk and T. Someya, Flexible organic transistors and circuits with extreme bending stability., *Nat. Mater.*, 2010, **9**, 1015–1022.
6 X. Qian, T. Wang and D. Yan, High mobility organic thin-film transistors based on p-p heterojunction buffer layer, *Appl. Phys. Lett.*, 2013, **103**, 6–10.
7 J. Takeya, M. Yamagishi, Y. Tominari, R. Hirahara, Y. Nakazawa, T. Nishikawa, T. Kawase, T. Shimoda and S. Ogawa, Very high-mobility organic single-crystal transistors with in-crystal conduction channels, *Appl. Phys. Lett.*, 2007, **90**, 2005–2008.
8 V. Podzorov, S. E. Sysoev, E. Loginova, V. M. Pudalov and M. E. Gershenson, Single-crystal organic field effect transistors with the hole mobility ~8 cm2/Vs, *Appl. Phys. Lett.*, 2003, **83**, 3504–3506.
9 V. C. Sundar, J. Zaumseil, V. Podzorov, E. Menard, R. L. Willett, T. Someya, M. E. Gershenson and J. a Rogers, Elastomeric Transistor Stamps : Transport in Organic Crystals, *Science*, 2004, **303**, 1644–1646.
10 M. Kytka, A. Gerlach, F. Schreiber and J. Kováč, Real-time observation of oxidation and photo-oxidation of rubrene thin films by spectroscopic ellipsometry, *Appl. Phys. Lett.*, 2007, **90**, 18–21.
11 S. Sinha, C. H. Wang, M. Mukherjee, T. Mukherjee and Y. W. Yang, Oxidation of rubrene thin films: An electronic structure study, *Langmuir*, 2014, **30**, 15433–15441.
12 E. Fumagalli, L. Raimondo, L. Silvestri, M. Moret, A. Sassella and M. Campione, Oxidation dynamics of epitaxial rubrene ultrathin films, *Chem. Mater.*, 2011, **23**, 3246–3253.
13 H. Najafov, D. Mastrogiovanni, E. Garfunkel, L. C. Feldman and V. Podzorov, Photon-assisted oxygen diffusion and oxygen-related traps in organic semiconductors, *Adv. Mater.*, 2011, **23**, 981–985.
14 S. Uttiya, L. Raimondo, M. Campione, L. Miozzo, A. Yassar, M. Moret, E. Fumagalli, A. Borghesi and A. Sassella, Stability to photo-oxidation of rubrene and fluorine-substituted rubrene, *Synth. Met.*, 2012, **161**, 2603–2606.
15 U. S. A. Force and T. Wilson, Excited Singlet Molecular Oxygen in Photooxidation, *J. Am. Chem. Soc.*, 1966, **23**, 2898–2902.
16 A. H. Williams, The photo-oxidation of hydrocarbon solutions, *Trans. Faraday Soc.*, 1939, **35**, 765–771.
17 R. M. Hochstrasser and M. Ritchie, The photoformation and thermal decomposition of rubrene peroxide, *Trans. Faraday Soc.*, 1956, **52**, 1363.
18 A. J. Maliakal, J. Y. C. Chen, W. Y. So, S. Jockusch, B. Kim, M. F. Ottaviani, A. Modelli, N. J. Turro, C. Nuckolls and A. P. Ramirez, Mechanism for oxygen-enhanced photoconductivity in rubrene: Electron transfer doping, *Chem. Mater.*, 2009, **21**, 5519–5526.
19 A. G. Leach and K. N. Houk, Diels-Alder and ene reactions of singlet oxygen, nitroso compounds and triazolinediones: transition states and mechanisms from contemporary theory., *Chem. Commun. Camb. Engl.*, 2002, 1243–1255.
20 D. Käfer and G. Witte, Growth of crystalline rubrene films with enhanced stability., *Phys. Chem. Chem. Phys. PCCP*, 2005, **7**, 2850–2853.
21 J.-M. Aubry, C. Pierlot, J. Rigaudy and R. Schmidt, Reversible Binding of Oxygen to Aromatic Compounds, *Acc. Chem. Res.*, 2003, **36**, 668–675.
22 J. Perronnet, Transformations of photoöxides in the naphthacene series, *Ann Chim Paris*, 1959, **4**, 365–462.
23 J. Perronnet, Properties of three oxonaphthacenes derived from the oxide of rubrene (5,6,11,12-tetraphenylnaphthacene), *Compt Rend*, 1955, **241**, 1474–1477.
24 J. Rigaudy, K. C. Nguyen and J. Y. Godard, Photochemical transformations of endoperoxides derived from polycyclic aromatic hydrocarbons. V. The rubrene endoperoxide case: formation of a new type of photoisomer, *Bull. Soc. Chim. Fr.*, 1985, 78–83.
25 T. N. Singh-Rachford and F. N. Castellano, Pd(II) phthalocyanine-sensitized triplet-triplet annihilation from rubrene., *J. Phys. Chem. A*, 2008, **112**, 3550–3556.
26 D. Koylu, S. Sarrafpour, J. Zhang, S. Ramjattan, M. J. Panzer and S. W. Thomas, Acene-doped polymer films: singlet oxygen dosimetry and protein sensing., *Chem. Commun. Camb. Engl.*, 2012, **48**, 9489–91.
27 T. Hosokawa, H. Nakano, K. Takami, K. Kobiro and A. Shiga, Acid-catalyzed transformation of rubrene to indenonaphthacene and its paired interacting orbital (PIO) analysis, *Tetrahedron Lett.*, 2003, **44**, 1175–1177.
28 Z. Margolin and F. A. Long, The Acidic Behavior of Chloroform, *J Am Chem Soc*, 1973, **2438**, 2757–2762.
29 A. Afzali, C. D. Dimitrakopoulos and T. L. Breen, High-Performance, Solution-Processed Organic Thin Film Transistors from a Novel Pentacene Precursor, *J. Am. Chem. Soc.*, 2002, **124**, 8812–8813.
30 A. Afzali, C. D. Dimitrakopoulos and T. O. Graham, Photosensitive Pentacene Precursor: Synthesis, Photothermal Patterning, and Application in Thin-Film Transistors, *Adv. Mater.*, 2003, **15**, 2066–2069.

View Article Online
DOI: 10.1039/C7TC05775J

31 K. P. Weidkamp, A. Afzali, R. M. Tromp and R. J. Hamers, A Photopatternable Pentacene Precursor for Use in Organic Thin-Film Transistors, *J. Am. Chem. Soc.*, 2004, **126**, 12740–12741.
32 A. Afzali, C. R. Kagan and G. P. Traub, N-sulfinylcarbamate-pentacene adduct: A novel pentacene precursor soluble in alcohols, *Synth. Met.*, 2005, **155**, 490–494.
33 D.-S. Kim, J. H. Kwon, S. Y. Cho, C. Lee, K.-S. Lee and T.-D. Kim, Organic field effect transistors fabricated using a composite of poly(9-vinylcarbazole) and pentacene precursor, *Synth. Met.*, 2011, **161**, 2422–2426.
34 K.-Y. Chen, H.-H. Hsieh, C.-C. Wu, J.-J. Hwang and T. J. Chow, A new type of soluble pentacene precursor for organic thin-film transistors, *Chem. Commun.*, 2007, **0**, 1065–1067.
35 T.-H. Chuang, H.-H. Hsieh, C.-K. Chen, C.-C. Wu, C.-C. Lin, P.-T. Chou, T.-H. Chao and T. J. Chow, Photogeneration and Thermal Generation of Pentacene from Soluble Precursors for OTFT Applications, *Org. Lett.*, 2008, **10**, 2869–2872.
36 C.-T. Chien, C.-C. Lin, M. Watanabe, Y.-D. Lin, T.-H. Chao, T. Chiang, X.-H. Huang, Y.-S. Wen, C.-H. Tu, C.-H. Sun and T. J. Chow, Tetracene -based field-effect transistors using solution processes, *J. Mater. Chem.*, 2012, **22**, 13070–13075.
37 M. Watanabe, Y. J. Chang, S.-W. Liu, T.-H. Chao, K. Goto, M. M. Islam, C.-H. Yuan, Y.-T. Tao, T. Shinmyozu and T. J. Chow, The synthesis, crystal structure and charge-transport properties of hexacene, *Nat. Chem.*, 2012, **4**, 574–578.
38 M. A. Fusella, F. Schreiber, K. Abbasi, J. J. Kim, A. L. Briseno and B. P. Rand, Homoepitaxy of Crystalline Rubrene Thin Films, *Nano Lett.*, 2017, **17**, 3040–3046.
39 H. M. Lee, H. Moon, H.-S. Kim, Y. N. Kim, S.-M. Choi, S. Yoo and S. O. Cho, Abrupt heating-induced high-quality crystalline rubrene thin films for organic thin-film transistors, *Org. Electron.*, 2011, **12**, 1446–1453.
40 T. R. Fielitz and R. J. Holmes, Crystal Morphology and Growth in Annealed Rubrene Thin Films, *Cryst. Growth Des.*, 2016, **16**, 4720–4726.
41 J. J. Kim, H. M. Lee, J. W. Park and S. O. Cho, Patterning of rubrene thin-film transistors based on electron irradiation of a polystyrene dielectric layer, *J. Mater. Chem. C*, 2015, **3**, 2650–2655.
42 M. A. Fusella, S. Yang, K. Abbasi, H. H. Choi, Z. Yao, V. Podzorov, A. Avishai and B. P. Rand, Use of an Underlayer for Large Area Crystallization of Rubrene Thin Films, *Chem. Mater.*, 2017, **29**, 6666–6673.
43 N. Stingelin-Stutzmann, E. Smits, H. Wondergem, C. Tanase, P. Blom, P. Smith and D. de Leeuw, Organic thin-film electronics from vitreous solution-processed rubrene hypereutectics, *Nat. Mater.*, 2005, **4**, 601–606.
44 P. S. Jo, D. T. Duong, J. Park, R. Sinclair and A. Salleo, Control of Rubrene Polymorphs via Polymer Binders: Applications in Organic Field-Effect Transistors, *Chem. Mater.*, 2015, **27**, 3979–3987.